Evaluation of helper-dependent canine adenovirus vectors in a 3D human CNS model

Daniel Simão[1,2], Catarina Pinto[1,2], Paulo Fernandes[1,2], Christopher J. Peddie[3], Stefania Piersanti[4], Lucy M. Collinson[3], Sara Salinas[5,6], Isabella Saggio[4,7,8], Giampietro Schiavo[3,9], Eric J. Kremer[5,6], Catarina Brito[1,2,§], Paula M. Alves[1,2]

[1]iBET - Instituto de Biologia Experimental e Tecnológica, Apartado 12, 2780-901 Oeiras, Portugal
[2]Instituto de Tecnologia Química e Biológica, Universidade Nova de Lisboa, Av. da República, 2780-157 Oeiras, Portugal
[3]Cancer Research UK London Research Institute, Lincoln's Inn Fields Laboratories, 44 Lincoln's Inn Fields, London WC2A 3LY, United Kingdom
[4]Dipartimento di Biologia e Biotecnologie “Charles Darwin”, Università di Roma La Sapienza, Piazzale Aldo Moro 5, 00185 Rome, Italy
[5]Institut de Génétique Moléculaire de Montpellier, CNRS 5535, 1919 Route de Mende, 34293 Montpellier,, France
[6]Université Montpellier, 34293 Montpellier, France
[7]Istituto Pasteur Fondazione Cenci Bolognetti, Università di Roma La Sapienza, Stanza 3-13, Piano 2, Piazzale Aldo Moro nº5, 00185 Rome, Italy
[8]Istituto di Biologia e Patologia Molecolari del CNR, Università di Roma La Sapienza, Piazzale Aldo Moro 5, 00185 Rome, Italy
[9]Sobell Department of Motor Neuroscience and Movement Disorders, Institute of Neurology, University College London, Gower Street, London WC1E 6BT, UK

[§]Corresponding author

Abstract

Background

Gene therapy is a promising approach with enormous potential for treatment of neurodegenerative disorders. Viral vectors derived from canine adenovirus type 2 (CAV-2) present attractive features for gene delivery strategies in the human brain, by preferentially transducing neurons, are capable of efficient axonal transport to afferent brain structures, have a 30-kb cloning capacity and have low innate and induced immunogenicity in humans. For clinical translation, in-depth pre-clinical evaluation of efficacy and safety in a human setting is primordial. Stem cell-derived human neural cells have a great potential as complementary tools by bridging the gap between animal models, which often diverge considerably from human phenotype, and clinical trials.

Methods

Herein, we explore helper-dependent CAV-2 (hd-CAV-2) efficacy and safety for gene delivery in a human stem cell-derived 3D neural *in vitro* model. Assessment of hd-CAV-2 transduction was performed at different multiplicities of infection, by evaluating transgene expression and impact on cell viability, ultrastructural cellular organization and neuronal gene expression.

Results

Under optimized conditions, hd-CAV-2 transduction led to stable long-term transgene expression with minimal toxicity. The evaluation of vector tropism showed that hd-CAV-2 preferentially transduces neurons, in contrast to human adenovirus type 5 (HAdV5) that showed increased tropism towards glial cells.

Conclusions

This work demonstrates, in a physiologically relevant 3D model, that hd-CAV-2 vectors are efficient vehicle for gene delivery to human neurons, with stable long-term transgene expression and minimal cytotoxicity.

Background

Neurodegenerative diseases, typically characterized by a progressive nervous system dysfunction, represent a heavy disease burden both in terms of patient suffering and economic cost. The prevalence of neurologic disorders has dramatically increased over the last decades and continues to increase, mainly due to higher life expectancy of populations, which elicits the urgent need for effective therapeutics [1].

With the increasing knowledge on the etiology of these disorders, several genetic mutations have been linked with the sporadic and familial forms of disease. The identification of these mutations can provide not only significant insights in the molecular mechanisms involved in the disease onset and progression, but also promising therapeutic targets for alternative approaches to the traditional pharmacological therapies, such as gene therapy [2]. Briefly, most gene delivery approaches have focused either on enzyme replacement, by restoring the enzymatic capacity of the affected brain regions, or on delivery of neurotrophic factors, to prevent the progression of the neurodegeneration process [3].

Over the last decades multiple non-viral gene delivery vehicles have been explored, nevertheless viral vectors are still the most efficient tools for *in vivo* gene transfer. The array of viral vector systems offers unique strengths, while presenting specific drawbacks [4, 5]. Therefore, thorough evaluation is required for selection of the optimal vector system for central nervous system (CNS) gene delivery. Most neurological disorders only affect a specific cell type, as is the case of the dopaminergic neurons of the nigrostriatal pathway in Parkinson's disease (PD) [6]. Thus, in addition to high transduction efficiency, vector tropism is of paramount importance to achieve targeted therapeutic gene delivery to the affected cells of a confined brain region, minimizing off-target transduction. Additionally, an ideal vector should be able to sustain long-term expression of the transgene with a single treatment, to maximize the therapeutic effect and minimize repeated dosage. Most importantly, the vector selection must guarantee the safety of the patient and avoid host immune responses or cytotoxicity, which may also hinder the therapeutic effect. Finally, it is important to consider the vector manufacture methods, which should be scalable and allow high titers along with high purity and concentration [5, 7, 8].

Recombinant adeno-associated viruses (AAV) have been the most widely used and studied vectors for gene delivery in the CNS and peripheral nervous system. The variety

of AAV identified serotypes enables the mixing of viral genomes and capsids creating mosaic "pseudotypes" which display a wide range of neural tropisms and efficacies, along with low pathogenicity and immunogenicity [5, 9]. However, AAV vectors display a low cloning capacity (≈4-6 kb), which limits their use in some applications. Recombinant adenoviruses (AdV) are an attractive alternative, due to a large cloning capacity (8-30 kb) and long-term transgene expression [5, 9], being the most explored platform in clinical trials worldwide (http://www.wiley.com/legacy/wileychi/genmed/clinical). Nonetheless, the toxicity and immunogenicity of some Ad types have been widely described [5, 7, 9], limiting the therapeutic efficacy. Non human viral vectors, such as canine adenovirus type 2 (CAV-2) derived vectors emerged as an alternative to human rAdV (HAdV), mainly due to lack of immunological memory [10]. Moreover, CAV-2 vectors preferentially transduce neurons in the rodent brain and in human organotypic cultures, along with efficient biodistribution via axonal retrograde transport in neurons [11, 12]. The development of helper-dependent CAV-2 vectors (hd-CAV-2) [13, 14] improved the efficiency and duration of transgene expression, minimizing the adaptive cell-mediated immune response [13]. hd-CAV-2 vectors have a cloning capacity of 30 kb [13] and allow stable transgene levels over 1 year in immunocompetent rat brain without immunosuppression [15]. During viral vector development, preclinical testing is crucial to evaluate both efficacy and safety, while understanding vector-cell interactions. Although the traditional primary cultures of rodent brain cells and animal models provide valuable data, these models too often diverge considerably from the human phenotype [16], thus not accurately predicting the clinical trials' outcome. In this context, stem cell-derived human neural cells, along with three dimensional (3D) culture systems, have great potential as complementary tools in pre-clinical research, bridging the gap between human clinical studies and animal models [16, 17]. We previously reported the development of a 3D neural cell model based on the differentiation of human midbrain-derived neural progenitor cells (hmNPC) as neurospheres, in a dynamic culture system [18, 19]. Differentiated neurospheres contain glial cells, oligodendrocytes and functional neurons, with enrichment in the dopaminergic phenotype.

In this study, we took advantage of the 3D neural *in vitro* model [18, 19] to evaluate hd-CAV-2 vectors gene delivery efficiency and cytotoxicity, For this we made use of a reporter eGFP-expressing hd-CAV-2, which can be produced in a robust and scalable bioprocess [20, 21], compatible with pre-clinical and clinical applications. Assessment

of hd-CAV-2 transduction was performed at different MOIs, by evaluation of transgene expression and toxicity by cell viability, impact on neuronal gene expression and ultrastructural cell organization. Under optimized conditions hd-CAV-2 transduction led to stable long-term transgene expression with low toxicity. This study demonstrates, in a physiologically relevant human *in vitro* model, that hd-CAV-2 vectors are efficient vehicle for gene transfer for human neurons and can be envisaged for treatment of neurodegenerative diseases, such as PD.

Methods

hmNPC expansion and differentiation

Human midbrain-derived neural progenitor cells (hmNPC) derived from aborted fetal brain tissue 12 to 14 weeks post-fertilization [18, 22] were kindly provided by Dr. Johannes Schwarz (Technical University of Munich, Germany). Tissue was obtained with mother's consent and in accordance with the Ethics Committee of the University of Leipzig and the German state and federal laws. Expansion and differentiation of hmNPC was performed as previously described [18, 19].

Viral stock production

hd-CAV-2 are vectors derived from CAV-2 strain Toronto A 26/61, GenBank J04368, containing an eGFP expression cassette. hd-CAV-2 stocks were produced by infection of E1-complementing dog kidney cells expressing Cre recombinase (DKCre) and purified by CsCl gradients, as previously described [23, 24]. Stocks titration were performed by infectivity assay for number of infectious particles/mL (ip/mL) [20, 25]. The obtained preps had a pp/ip unit ratio of 100:1. HAdV5 vectors used are E1-deleted adenovirus type 5, expressing green fluorescent protein as transgene (HAdV5-GFP), which were produced according to previous reports [25]. In this study, multiplicity of infection (MOI) is determined by the number of infectious viral particles per cell (ip/cell).

Transduction

Following hmNPC neurospheres differentiation, transduction was performed with 50% reduction of the working volume. Total cell number was determined by counting cell nuclei using a Fuchs-Rosenthal hemacytometer after digestion with lysis buffer (0.1 M citric acid, 1% Triton X-100 (w/w) and 0.1% crystal violet (w/v)) [26]. At 4 hours post-

transduction a complete media exchange was performed. Neurospheres were maintained in culture up to 30 days post-transduction, with a 75% medium exchange performed every 3 days.

Cell viability

Cell viability was assessed using the metabolic indicator PrestoBlue™ (Invitrogen), according to the manufacture's recommendation. Briefly, neurospheres were plated on poly-L-ornithine-fibronectin (PLOF)-coated multi-well plates and allowed to attach for 2 hours. Cells were incubated with fresh medium containing 10% (v/v) PrestoBlue, for 2 hours. Supernatant's fluorescence was measured in 96-well plates using a microwell plate fluorescence reader (FluoroMax-4, Horiba JobinYvon) and neurospheres were harvested for total protein quantification, using the Micro BCA Protein Assay Kit (Pierce). Fluorescence intensity was normalized for total protein and evaluated relatively to control (MOI 0).

Fluorescence microscopy

Neurospheres were plated on PLOF-coated glass coverslips and allowed to attach for 2 days, fixed in 4% (w/v) paraformaldehyde (PFA) + 4% (w/v) sucrose in PBS for 30 min and processed for immunostaining as previously described[27]. Primary and secondary antibodies were used as follows: mouse anti-βIII-tubulin (1:200; Millipore); mouse anti-GFP (1:200; Sigma-Aldrich); rabbit anti-TH (1:100; Santa Cruz); rabbit anti-GFAP (1:200; Millipore); rabbit anti-CAR (1:200; gift from Joseph Zabner), mouse anti-CAR (1:200; Millipore); AlexaFluor® 488 goat anti-mouse IgG and AlexaFluor® 594 goat anti-rabbit IgG (1:500; Invitrogen). Cell nuclei were counterstained with DAPI or TO-PRO-3 (Invitrogen). Samples were visualized using point scan confocal (SP5, Leica) or multi-photon (Ultima, Prairie) microscopy. Merge between channels and maximum z-projections, as well as linear brightness and contrast adjustments of the images, were performed using the open source ImageJ software.

Electron microscopy

Neurospheres were fixed in 2.5% (w/v) glutaraldehyde and 4% (w/v) formaldehyde in 0.1 M phosphate buffer (pH 7.4) and then processed for serial blockface scanning electron microscopy (SBF SEM). Samples were embedded in Durcupan resin following the method of NCMIR [28]. Small groups of neurospheres were mounted on pins and trimmed for SBF SEM. Images were acquired using a 3View2XP (Gatan)) attached to a

Sigma VP SEM (Zeiss), at a resolution of 8,192 x 8,192 pixels (horizontal frame width of 64.29 µm; pixel size of 7.8 nm) with 2 µs dwell time and 35 nm slice thickness. SEM was operated in high vacuum, with high current mode active, at an indicated magnification of 4,000. The 20 µm aperture was used, at an accelerating voltage of 1.4 kV (hd-CAV-2 transduced) or 1.2 kV (control). Alignment of the image stack was accomplished using the 'Register virtual stack slices' plugin in Fiji [29], with translation based extraction and registration models to minimise distortion of the dataset. Aligned image stacks were then calibrated for pixel dimensions. Movies were generated using Amira (FEI Visualization Sciences Group) and Quicktime Pro, showing 500 slices from the centre of each dataset (total dataset for hd-CAV-2 transduced = 1,450 slices, representing a total volume of 209,760 μm^2; total dataset for control = 533 slices, representing a total volume of 77,105 μm^2).

qRT-PCR

Total RNA was extracted with High Pure RNA Isolation Kit (Roche), according to the manufacturer's instructions. RNA was quantified in a NanoDrop 2000c (Thermo Scientific) and used for cDNA synthesis. Reverse transcription was performed with High Fidelity cDNA Synthesis Kit (Roche), using Anchored-oligo(dT)18 Primer (Roche) or with the Super Script III First Strand synthesis system (Invitrogen), using random hexamers (Invitrogen). qPCRs were performed in triplicates using LightCycler 480 SYBR Green I Master Kit (Roche) with the following primers: eGFP (GFP fwd 5'-CAACAGCCACAACGTCTATATCATG-3' and GFP rev 5'-ATGTTGTGGCGGATCTTGAAG-3'), tyrosine hydroxylase (TH fwd 5'-AGCCCTACCAAGACCAGACG-3' and TH rev 5'-GCGTGTACGGGTCGAACTT-3'), synapsin II (SYN2 fwd 5'-TGGAACAGGCAGAATTTTCA-3' and SYN2 rev 5'-GGACAACCTTTGTGCCATTC-3') and ribosomal protein L22 (RPL22 fwd 5'-CACGAAGGAGGAGTGACTGG-3' and RPL22 rev 5'-TGTGGCACACCACTGACATT-3'). As alternative TaqMan Universal PCR Master Mix (Applied Biosystems), and the following TaqMan® Gene Expression Assays (Applied Biosystems): *TRKA* (ID: Hs01021011_m1); *TRKB* (ID: Hs00178811_m1); *TRKC* (ID:Hs00176797_m1); *RET* (ID:Hs01120030_m1); *DDC* (ID: Hs01105048_m1); *QDPR* (ID: Hs00165610_m1), *GCH1* (ID: Hs00609198_m1); *DRD2* (ID: Hs00241436_m1); *SYT1* (ID: Hs00194572_m1); *SYP* (ID: Hs00300531_m1); *SYNPO* (ID: Hs00702468_s1); *PSD95* (ID: Hs00176354_m1); *vGAT* (ID: Dm01823909_g1).

The reactions were performed with Applied Biosystems 7300 Real Time PCR system or LightCycler 480 Instrument II 96-well block (Roche). Quantification cycle values (Cq's) and melting curves were determined using LightCycler 480 Software version 1.5 (Roche). All data were analyzed using the $2^{-\Delta\Delta Ct}$ method for relative gene expression analysis [30]. Changes in gene expression were normalized using the housekeeping gene *RPL22* (ribosomal protein L22) as internal control. Statistical analysis was carried out using GraphPad Prism 5 software.

Results

hd-CAV-2 impact on cell viability and neuronal population

To determine the most suitable transduction parameters, three multiplicities of infection (MOI) were tested on the human 3D neural model (Figure 1A). We assessed gene delivery efficiency, by evaluating transgene expression levels, and cytotoxic effects exerted by the vectors, by measuring cell viability and expression levels of neuronal/synaptic markers. The different MOIs evaluated (20, 50 and 100 infectious particles/cell) were selected based on data previously generated with an E1-deleted CAV-2 vector expressing GFP [18]. Neurosphere transduction showed an increase in transgene mRNA levels according to the MOI increase, with a 3- and 4.5-fold increase (relatively to MOI 20) for MOI 50 and 100, respectively, at 5 days post-transduction (dpt) (Figure 1B). In agreement with these observations, the fraction of GFP-positive cells also increased with the MOI, as observed by confocal microscopy (Figure 1C).
Cytotoxicity assessment showed no significant decrease in cell viability for MOI 50 and 100, relatively to control (Figure 1D). Moreover, no significant modulation in the pre-synaptic marker synapsin II (*SYN2*) gene expression was observed for the different MOIs (Figure 1E). Still, a 4-fold decrease in the expression of the dopaminergic marker tyrosine hydroxylase (*TH)* was observed for MOI 100 at 5 dpt, relatively to the neurospheres before hd-CAV-2 transduction. These results suggest that higher hd-CAV-2 MOIs, although allowing higher gene delivery efficiency, can affect specific neuronal populations, such as dopaminergic neurons. These observations emphasize the need for a careful MOI assessment in pre-clinical studies to identify toxic effects, while sustaining an efficient gene delivery to target cells. In this study, considering the level of transgene expression and the absence of modulation for the neuronal markers

evaluated, MOI 20 and 50 were selected for further characterization of hd-CAV-2 transduction.

The impact of hd-CAV-2 transduction on the neurospheres was further addressed by analyzing the expression of an enlarged set of neuronal markers (Figure 2), comprising neurotrophic receptors (*TrkA, TrkB, TrkC* and *RET*), dopamine biosynthesis pathway enzymes (*DDC, QDPR, GCH1*), dopamine receptor (*DRD2*), pre-synaptic (*SYT1*, *SYP*, *SYNPO* and *vGAT*) and post-synaptic (*PSD95*) proteins. Compared with the control (MOI 0), a MOI of 20 or 50 for hd-CAV-2 transduction did not induce significant modulation on the evaluated markers. Thus, given the 3-fold increase in transgene expression with MOI 50 (Figure 1B) and the comparable low cytotoxic effects, the MOI 50 was selected for more comprehensive studies addressing the impact of hd-CAV-2 transduction on ultrastructural cell organization, vector tropism and duration of transgene expression.

hd-CAV-2 impact on ultrastructural cell organization

Cellular ultrastructure was analyzed both for transduced (MOI 50) and non-transduced neurospheres by serial blockface scanning electron microscopy (SBF SEM). The obtained image stacks showed similar numbers and spatial distribution of cell bodies, as well as the complexity of the extending neuronal processes network. Moreover, comparable cellular ultrastructural details within non-transduced and transduced cells were observed, including clearly defined mitochondria, Golgi stacks, endoplasmic reticulum and other subcellular structures. Altogether, these results suggest that hd-CAV-2 transduction did not induced noticeable structural alterations on human neural cells within the neurospheres.

hd-CAV-2 tropism and long-term transduction dynamics

hd-CAV-2 preferential transduction of neurons in rodent models has been previously linked with the expression of coxsackievirus and adenovirus receptor (CAR) [11, 12, 31]. Given this, we analyzed the expression and distribution of CAR on human neurospheres by confocal microscopy. This revealed that CAR was highly expressed in neurons, co-localizing with βIII-tubulin-positive cells, but not in glial cells, where low co-localization with GFAP-positive cells was observed (Figure 4A). To further explore the interaction between CAV-2 vectors and human neurons, we then incubated

neurospheres with fluorescently labeled CAV-2 particles (CAV-Cy3), followed by immunofluorescence labeling of neurons (βIII-tubulin). This resulted in a high density of CAV-Cy3 particles detected along neuronal cells (Figure 4B), indicating that these vectors were able to recognize these cells, both in soma and branching processes, for attachment and internalization.

For a more detailed study on the tropism of hd-CAV-2 in human neural cells, we then compared the phenotype of hd-CAV-2 transduced cells to a vector derived from human adenovirus type 5 (HAdV5), which has been widely explored for gene therapy strategies [32, 33]. Differences both in terms of morphology and distribution of transduced cells along the neurospheres' volume were observed (Figure 4C). For hd-CAV-2, the typical morphology of transduced cells was neuronal-like, with long processes extending from the soma. By contrast, HAdV5-transduced cells presented glial-like morphology, with larger cytoplasmic volume and no extension of cell processes. Interestingly, upon hd-CAV-2 transduction, it was possible to identify multiple GFP-positive cells across different layers towards the inner core of the neurospheres, which was evidenced by a depth lookup table (Figure 4C). Sections on the surface were plotted in blue progressing to green and red/pink across a 41 μm volume depth. On the other hand, upon HAdV5 transduction, the presence of GFP-positive cells was restricted to the neurospheres' surface, presenting a radial pattern from blue cells in the center towards red/pink cells only in the periphery.

To confirm the different identity of hd-CAV-2 and HAdV5 transduced cells, different neural lineages were identified by immunodetection: TH for dopaminergic neurons and GFAP for glia lineages (Figure 4D). This revealed that hd-CAV-2 were able to efficiently transduce dopaminergic neurons (TH-positive cells), while poorly transducing glial cells (GFAP-positive cells), consistent with CAR expression on neurons. By contrast, HAdV5 preferentially transduced glial cells.

In addition to tropism, we also analyzed the dynamics of transgene expression. Following hd-CAV-2 or HAdV5 transduction, neurospheres were maintained for at least 30 dpt, presenting high cell viability. Both vectors were able to sustain the expression of the transgene during this culture time (Figure 5). hd-CAV-2 maintained stable *eGFP* expression levels over the 30 dpt, while HAdV5 transduction led to a 2-fold increase during the first 21 dpt followed by a decrease at 30 dpt to similar levels as observed at 5 dpt. Moreover, *TH* expression dynamics revealed no significant differences between the two vectors during the 30 dpt, suggesting low long-term

cytotoxic effects of viral transduction on dopaminergic neuronal population for the selected MOI.

Discussion

Previous reports on rodents showed the efficiency of CAV-2 vectors in transducing neurons, with the ability to sustain long-term transgene expression and being retrogradely transported in neurons, while maintaining low levels of immunogenicity [12, 15]. Given the fundamental differences between rodent and human cells, it is critical to demonstrate the efficacy and safety of such vectors in human cells in early stages of development. In this work, we explored an established human 3D *in vitro* CNS model based on differentiation of hmNPC for pre-clinical testing of hd-CAV-2 vectors. During differentiation, these cells recapitulate the specific midbrain developmental programs, resulting in a human cell model enriched in functional dopaminergic neurons [19].

Here, we found that hd-CAV-2 vectors efficiently transduce human neural cells. The screening detected cytotoxic effects associated with high vector MOIs (100 ip/cell). These effects were more evident on the dopaminergic population, as determined by a significant decrease in *TH* expression levels and no modulation on synaptic gene *SYN2*. Notably, differential hd-CAV-2 transduction efficacy has also been observed in the rodent brain, where the higher efficiency was observed for dopaminergic neurons, followed by noradrenergic neurons and the least efficient transduction was observed for serotonergic neurons (unpublished data). Moreover, dopaminergic neurons have been previously reported to be more susceptible to GFP toxicity, relative to other neuronal populations [34]. In this study, transduction of rodent brain with high doses of an AAV8-GFP vector induced a significant loss in TH^+ neurons compared to an empty vector. By contrast, no loss of pyramidal or granular neurons was observed in the hippocampus. Together, these data indicate different transduction efficiencies or transgene related effects in different neuronal subtypes, which can lead to differential survival.

To confirm the absence of cytotoxicity for the low and mid MOIs (20 and 50 ip/cell), expression of a larger panel of neuronal genes, including neurotrophic receptors, dopamine biosynthesis pathway enzymes, dopamine receptors and synaptic proteins was evaluated at 5 dpt. Here, no significant changes were observed for both MOIs in

comparison with the control. These results are in accordance with data on the toxicogenomic profile of hd-CAV-2 transduction of 2D hmNPC cultures, showing no significant vector-induced modulation of the neuron morphogenesis pathways and an activation of pro-survival genes [35]. Moreover, hd-CAV-2 transduction of neurospheres (MOI 50) did not induce noticeable structural alterations, neither at cells spatial distribution within neurospheres nor at cellular ultrastructural level.

These results show the importance of MOI screening and optimization to attain efficient levels of gene delivery, while maintaining cytotoxic effects to a minimal. Nevertheless, when considering an *in vivo* setting, one must not exclude possible immunological complications often associated with a diseased brain and gene transfer vectors, which in case of AdV are related with innate and memory immunity to the wild-type pathogen. This can lead to adverse side effects upon administration, such as acute inflammatory reactions, posing a safety risk for the patient. Still, previous reports have shown negligible levels of neutralizing CAV-2 antibodies in healthy humans [23], as well as lower immunogenicity than HAdV in immunologically naïve rodents [15, 36]. As with all vectors, this should be a matter of careful scrutiny in potential clinical trials to ensure patient safety and the success of therapy. Moreover, data obtained from rodents may not accurately reflect the human setting. A recent study showed that HAdV5 and murine coagulation factor X (FX) complexes stimulated an innate inflammatory response via Toll-like receptor 4 in murine macrophages [37]. However, HAdV5 and human FX complexes do not stimulate an innate response in human mononuclear phagocytes [38].

Our results showed in a 3D human cell model that hd-CAV-2 vectors preferentially transduce neurons rather than glial cells, in agreement with previous reports on animal models and *ex vivo* human brain slices [12, 15]. Transduction with HAdV5 resulted in preferential glial transduction, further confirming the distinct vector tropism between CAV-2 and human types. Thus, in spite of sharing many characteristics such as a very similar capsid structure and genomic organization [39], these vectors display clearly different tropisms. The molecular basis for CAV-2 neuronal tropism vs. HAdV5 likely relies on the exclusive binding to CAR for internalization, due to absence of an integrin-interacting motif (e.g. RGD motif), reducing the possibility of vector internalization via $\alpha_M\beta_2$ integrins [31]. Hence, CAR expression is essential for CAV-2 transduction, which in this human model was restricted to the neuronal population, in agreement with previous reports in rodent models [12]. Thus, our results in a human context further support the CAR-dependent CAV-2 binding and internalization hypothesis, which leads

to increased neuronal tropism of CAV-2 and poor glia transduction. Moreover, our results showed a clear accumulation of CAV-Cy3 particles along neuronal processes, which indicates that CAV-2 vectors can bind and be internalized along these processes and not only in the soma. This may also suggest a similar trafficking mechanism as previously reported for murine primary neurons, where after vector binding to CAR and subsequent internalization, CAV-2 vectors are transported via axonal trafficking, which was proposed to be dictated by an innate CAR trafficking mechanism [11, 40].

In addition to CAV-2 tropism, one can further explore strategies for neuronal specific transgene expression, such as neuronal specific promoters [41, 42], which can reduce even more potential off target transduction and/or restrict transgene expression to a neuronal subpopulation (e.g. dopaminergic neurons).

Conclusions

This work demonstrates, in a physiologically relevant 3D model, that hd-CAV-2 vectors are efficient vehicles for gene transfer to human neurons, with stable long-term transgene expression and minimal cytotoxicity. Moreover, in the long term, this study addresses the potential of hd-CAV-2 vectors for gene therapy of human neurodegenerative diseases, such as PD, further supporting the valuable data previously obtained from pre-clinical animal models.

Authors' contributions

DS designed, performed experiments and prepared the manuscript. CP performed experiments and contributed to manuscript writing. PF produced the hd-CAV-2 stocks used in the work. SP and IS generated the neuronal gene expression data. CJP and LMC carried out the electron microscopy and GS supervised its analysis. SS contributed to CAR analysis, CAV-Cy3 experiments and critically revised the manuscript. EJK, GS gave conceptual advice and critically revised the manuscript. CB and PMA designed the study and CB supervised the work and manuscript writing. All authors discussed the results and commented on the manuscript.

Acknowledgements

We gratefully acknowledge Dr. Johannes Schwarz for the supply of hmNPC within the scope of the EU project BrainCAV (FP7-222992). This work was supported by BrainCAV (FP7-222992) and Brainvectors (FP7-286071), funded by the EU, PTDC/EBB-BIO/112786/2009 and PTDC/EBB-BIO/119243/2010, funded by Fundação para a Ciência e Tecnologia, Portugal and Cancer Research UK. DS, ACP and PF were recipients of a PhD fellowship from FCT, Portugal (SFRH/BD/78308/2011, PD/BD/52202/2013 and SFRH/BD/70810/2010, respectively).

References

1. Forman MS, Trojanowski JQ, Lee VM: **Neurodegenerative diseases: a decade of discoveries paves the way for therapeutic breakthroughs.** *Nat Med* 2004, **10**:1055–63.

2. Ulusoy A, Kirik D: **Development of advanced therapies based on viral vector-mediated overexpression of therapeutic molecules and knockdown of disease-related genes for Parkinson's disease**. *Ther Deliv* 2011, **2**:37–50.

3. Björklund T, Kirik D: **Scientific rationale for the development of gene therapy strategies for Parkinson's disease.** *Biochim Biophys Acta* 2009, **1792**:703–13.

4. Gan Y, Jing Z, Stetler RA, Cao G: **Gene delivery with viral vectors for cerebrovascular diseases**. *Front Biosci (Elite Ed)* 2013, **5**:188–203.

5. Lentz TB, Gray SJ, Samulski RJ: **Viral vectors for gene delivery to the central nervous system.** *Neurobiol Dis* 2012, **48**:179–88.

6. Toulouse A, Sullivan AM: **Progress in Parkinson's disease-where do we stand?**. *Prog Neurobiol* 2008, **85**:376–92.

7. Gray SJ, Woodard KT, Samulski RJ: **Viral vectors and delivery strategies for CNS gene therapy.** *Ther Deliv* 2010, **1**:517–34.

8. Feng LR, Maguire-zeiss KA: **Gene Therapy in Parkinson's Disease: Rationale and Current Status**. *CNS Drugs* 2010, **24**:177–192.

9. Manfredsson FP, Mandel RJ: **Development of gene therapy for neurological disorders**. *Discov Med* 2010, **9**:204–211.

10. Perreau M, Kremer EJ: **The conundrum between immunological memory to adenovirus and their use as vectors in clinical gene therapy.** *Mol Biotechnol* 2006, **34**:247–256.

11. Salinas S, Bilsland LG, Henaff D, Weston AE, Keriel A, Schiavo G, Kremer EJ: **CAR-associated vesicular transport of an adenovirus in motor neuron axons.** *PLoS Pathog* 2009, **5**:e1000442.

12. Soudais C, Laplace-Builhe C, Kissa K, Kremer EJ: **Preferential transduction of neurons by canine adenovirus vectors and their efficient retrograde transport in vivo.** *FASEB J* 2001, **15**:2283–2285.

13. Bru T, Salinas S, Kremer EJ: **An Update on Canine Adenovirus Type 2 and Its Vectors**. *Viruses* 2010, **2**:2134–2153.

14. Soudais C, Skander N, Kremer EJ: **Long-term in vivo transduction of neurons throughout the rat CNS using novel helper-dependent CAV-2 vectors**. *FASEB J* 2004, **18**:391–3.

15. Soudais C, Skander N, Kremer EJ: **Long-term in vivo transduction of neurons throughout the rat CNS using novel helper-dependent CAV-2 vectors.** *FASEB J* 2004, **18**:391–393.

16. Schüle B, Pera R a R, Langston JW: **Can cellular models revolutionize drug discovery in Parkinson's disease?**. *Biochim Biophys Acta* 2009, **1792**:1043–51.

17. Pampaloni F, Reynaud EG, Stelzer EHK: **The third dimension bridges the gap between cell culture and live tissue.** *Nat Rev Mol Cell Biol* 2007, **8**:839–845.

18. Brito C, Simão D, Costa I, Malpique R, Pereira CI, Fernandes P, Serra M, Schwarz SC, Schwarz J, Kremer EJ, Alves PM: **3D cultures of human neural progenitor cells: dopaminergic differentiation and genetic modification.** *Methods* 2012, **56**:452–60.

19. Simão D, Pinto C, Piersanti S, Weston A, Licursi V, Collinson L, Salinas S, Serra M, Teixeira AP, Schwarz S, Saggio I, Kremer EJ, Schiavo G, Brito C, Alves PM: **Modeling human neural functionality in vitro: 3D culture for dopaminergic differentiation**. *Tissue Eng Part A* 2015, **21**:654–668.

20. Fernandes P, Peixoto C, Santiago VM, Kremer EJ, Coroadinha AS, Alves PM: **Bioprocess development for canine adenovirus type 2 vectors.** *Gene Ther* 2013, **20**:353–60.

21. Fernandes P, Simão D, Guerreiro MR, Kremer EJ, Coroadinha a S, Alves PM: **Impact of adenovirus life cycle progression on the generation of canine helper-dependent vectors**. *Gene Ther* 2015, **22**:40–49.

22. Storch A, Paul G, Csete M, Boehm BO, Carvey PM, Kupsch A, Schwarz J: **Long-term proliferation and dopaminergic differentiation of human mesencephalic neural precursor cells.** *Exp Neurol* 2001, **170**:317–325.

23. Kremer EJ, Boutin S, Chillon M, Danos O: **Canine Adenovirus Vectors□: an Alternative for Adenovirus-Mediated Gene Transfer**. *J Virol* 2000, **74**:505–512.

24. Fernandes P, Santiago VM, Rodrigues AF, Tomás H, Kremer EJ, Alves PM, Coroadinha AS: **Impact of E1 and Cre on adenovirus vector amplification: developing MDCK CAV-2-E1 and E1-Cre transcomplementing cell lines**. *PLoS One* 2013, **8**:e60342.

25. Ferreira TB, Perdigão R, Silva AC, Zhang C, Aunins JG, Carrondo MJT, Alves PM: **293 cell cycle synchronisation adenovirus vector production.** *Biotechnol Prog* 2009, **25**:235–43.

26. Alves P, Moreira J, Rodrigues J, Aunins J, Carrondo M: **Two□dimensional versus three□dimensional culture systems: Effects on growth and productivity of BHK cells**. *Biotechnol Bioeng* 1996, **52**:429–432.

27. Serra M, Correia C, Malpique R, Brito C, Jensen J, Bjorquist P, Carrondo MJT, Alves PM: **Microencapsulation technology: a powerful tool for integrating expansion and cryopreservation of human embryonic stem cells.** *PLoS One* 2011, **6**:e23212.

28. Deerinck TJ, Bushong EA, Thor A, Ellisman MH: **NCMIR methods for 3D EM: a new protocol for preparation of biological specimens for serial block face scanning electron microscopy**. 2010.

29. Schindelin J, Arganda-Carreras I, Frise E, Kaynig V, Longair M, Pietzsch T, Preibisch S, Rueden C, Saalfeld S, Schmid B, Tinevez J-Y, White DJ, Hartenstein V, Eliceiri K, Tomancak P, Cardona A: **Fiji: an open-source platform for biological-image analysis.** *Nat Methods* 2012, **9**:676–82.

30. Livak KJ, Schmittgen TD: **Analysis of relative gene expression data using real-time quantitative PCR and the 2(-Delta Delta C(T)) Method.** *Methods* 2001, **25**:402–8.

31. Soudais C, Boutin S, Hong SS, Chillon M, Danos O, Bergelson JM, Boulanger P, Kremer EJ: **Canine Adenovirus Type 2 Attachment and Internalization□: Coxsackievirus-Adenovirus Receptor, Alternative Receptors, and an RGD-Independent Pathway**. *J Virol* 2000, **74**:10639–10649.

32. Ghosh SS, Gopinath P, Ramesh A: **Adenoviral vectors: a promising tool for gene therapy.** *Appl Biochem Biotechnol* 2006, **133**:9–29.

33. Räty JK, Pikkarainen JT, Wirth T, Ylä-Herttuala S: **Gene therapy: the first approved gene-based medicines, molecular mechanisms and clinical indications**. *Curr Mol Pharmacol* 2008, **1**:13–23.

34. Klein RL, Dayton RD, Leidenheimer NJ, Jansen K, Golde TE, Zweig RM: **Efficient neuronal gene transfer with AAV8 leads to neurotoxic levels of tau or green fluorescent proteins.** *Mol Ther* 2006, **13**:517–27.

35. Piersanti S, Astrologo L, Licursi V, Costa R, Roncaglia E, Gennetier A, Ibanes S, Chillon M, Negri R, Tagliafico E, Kremer EJ, Saggio I: **Differentiated**

neuroprogenitor cells incubated with human or canine adenovirus, or lentiviral vectors have distinct transcriptome profiles. *PLoS One* 2013, **8**:e69808.

36. Keriel A, René C, Galer C, Zabner J, Kremer EJ: **Canine Adenovirus Vectors for Lung-Directed Gene Transfer□: Efficacy , Immune Response , and Duration of Transgene Expression Using Helper-Dependent Vectors Canine Adenovirus Vectors for Lung-Directed Gene Transfer□: Efficacy , Immune Response , and Durat**. *J Virol* 2006, **80**:1487–1496.

37. Doronin K, Flatt JW, Di Paolo NC, Khare R, Kalyuzhniy O, Acchione M, Sumida JP, Ohto U, Shimizu T, Akashi-Takamura S, Miyake K, MacDonald JW, Bammler TK, Beyer RP, Farin FM, Stewart PL, Shayakhmetov DM: **Coagulation factor X activates innate immunity to human species C adenovirus.** *Science (80-)* 2012, **338**:795–8.

38. Eichholz K, Mennechet F, Kremer EJ: **Human coagulation factor X-adenovirus type 5 complexes poorly stimulate an innate immune response in human mononuclear phagocytes.** *J Virol* 2014(December).

39. Soudais C, Boutin S, Kremer EJ: **Characterization of cis-acting sequences involved in canine adenovirus packaging.** *Mol Ther* 2001, **3**:631–40.

40. Salinas S, Zussy C, Loustalot F, Henaff D, Menendez G, Morton PE, Parsons M, Schiavo G, Kremer EJ: **Disruption of the coxsackievirus and adenovirus receptor-homodimeric interaction triggers lipid microdomain- and dynamin-dependent endocytosis and lysosomal targeting.** *J Biol Chem* 2014, **289**:680–95.

41. Huang D, Desbois A, Hou ST: **A novel adenoviral vector which mediates hypoxia-inducible gene expression selectively in neurons**. *Gene Ther* 2005, **12**:1369–1376.

42. Namikawa K, Murakami K, Okamoto T, Okado H, Kiyama H: **A newly modified SCG10 promoter and Cre/loxP-mediated gene amplification system achieve highly specific neuronal expression in animal brains**. *Gene Ther* 2006, **13**:1244–1250.

Figures

Figure 1 - hd-CAV-2 transduction of differentiated human midbrain-derived neural precursor cells (hmNPC) neurospheres.

(A) Experimental design of cell differentiation and transduction. **(B)** Fold changes of *eGFP* expression for multiplicities of infection (MOI) 20, 50 and 100 infectious particles per cell (normalized to MOI 20). **(C)** Confocal microscopy of whole neurospheres. Maximum intensity z-projections of 38 (MOI 20) and 33 (MOI 50) optical sections of 1 µm. Scale bars, 100 µm. **(D)** Cell viability assessment, normalized for control (MOI 0). **(E)** Fold changes in tyrosine hydroxylase (*TH*) and synapsin II (*SYN2*) gene expression at 0 and 5 days post-transduction (dpt) (normalized for 0 dpt). Data are mean ± SEM of 3 independent experiments, asterisks indicate significant difference (*P < 0.05, **P < 0.01, ***P < 0.001) by a one-way ANOVA analysis with a Tukey's post-hoc multiple comparison test.

Figure 2 - Gene expression analysis of differentiated neurospheres transduced with hd-CAV-2.

Gene expression fold changes (normalized to control – MOI 0) of neurotrophic receptors (*TrkA*, *TrkB*, *TrkC* and *RET*), dopamine biosynthesis pathway enzymes (*DDC*, *QDPR*, *GCH1*), dopamine receptor (*DRD2*), pre-synaptic proteins (*SYT1*, *SYP*, *SYNPO* and *vGAT*) and post-synaptic protein (*PSD95*). Data are mean ± SEM of 3 independent experiments.

Figure 3 - hd-CAV-2 transduction impact on ultrastructural cell organization of differentiated neurospheres.

Electron micrographs extracted from the SBF SEM image stacks showing the internal structure of non-transduced **(A)** and transduced (**B**; MOI 50) neurospheres at 5 days post-transduction. Boxed areas (1, 2) highlight details of ultrastructure within each cell, including mitochondria (M), Golgi stacks (G), endoplasmic reticulum (ER), and other subcellular structures (N: nucleus, Np: nuclear pore). Scale bars – 5 µm (a, b), 1 µm (1, 2).

Figure 4 - Characterization of hd-CAV-2 and HAdV5 specific tropism.

(A) CAR immunofluorescence confocal microscopy of hd-CAV-2 and HAdV5 transduced neurospheres. Spatial distribution of transduced cells is highlighted by a depth lookup table. Maximum intensity z-projections of 41 optical sections of 1 µm, where blue indicates 0 µm and pink 41 µm. Inset depicts typical morphology of transduced cells. Scale bars, 50 µm. **(B)** Immunofluoresce microscopy of neurospheres incubated with CAV-Cy3 particles (red) stained for βIII-tubulin (green). Nuclei were labelled with TO-PRO3. Single optical section. Scale bar, 20 µm. **(C)** Immunofluoresce microscopy of neurospheres transduced with hd-CAV-2 and HAdV5, stained for TH and GFAP. Maximum intensity z-projections of 55 (TH – hd-CAV-2), 19 (TH – HAdV5), 42 (GFAP – hd-CAV-2) and 23 (GFAP – HAdV5) optical sections of 0.33 µm. Scale bars, 50 µm. **(D)** Immunofluoresce microscopy of neurospheres stained for CAR, βIII-tubulin and GFAP. Maximum intensity z-projections of 33 (βIII-tubulin) and 14 (GFAP) optical sections of 0.38 µm. Scale bars, 20 µm.

Figure 5 - hd-CAV-2 and HAdV5 transgene expression dynamics.

Gene expression fold changes of *eGFP* **(A)** and *TH* **(B)** expression in hd-CAV-2 and HAdV5 transduced neurospheres, along 30 dpt. Data are mean ± SEM of 2 independent experiments.

Additional files

Video S1 – Serial block-face scanning electron microscopy (SBFSEM) image stack of non-transduced neurospheres. The video scrolls through Z, X, and Y axes, respectively.

Video S2 – Serial block-face scanning electron microscopy (SBFSEM) image stack of transduced neurospheres (MOI 50). The video scrolls through Z, X, and Y axes, respectively.

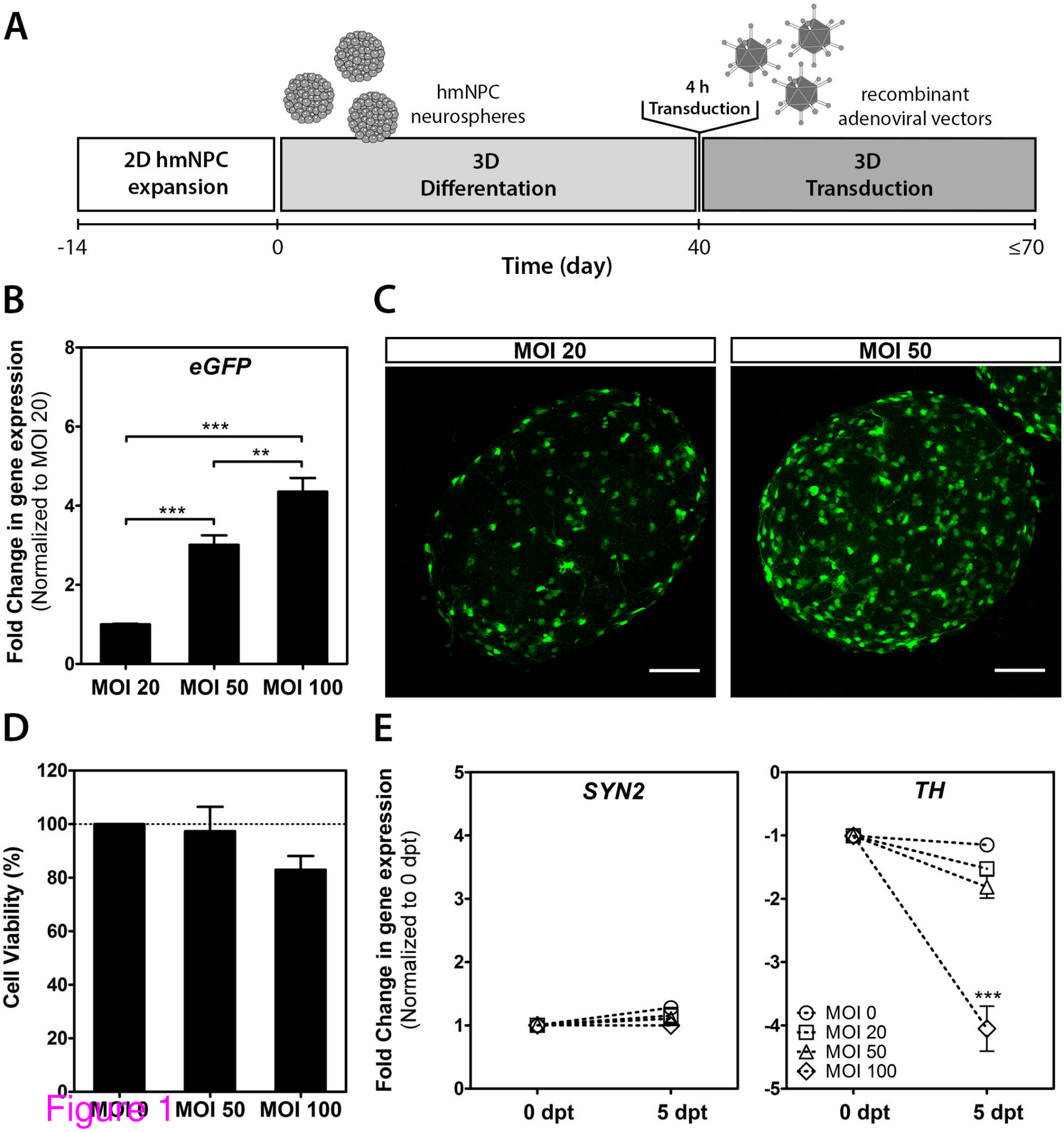
A
hmNPC
neurospheres
4 h
Transduction
recombinant
adenoviral vectors
2D hmNPC
expansion
3D
Differentation
3D
Transduction
-14
0
40
≤70
Time (day)
B
eGFP
Fold Change in gene expression
(Normalized to MOI 20)
***
**
***
MOI 20
MOI 50
MOI 100
C
MOI 20
MOI 50
D
Cell Viability (%)
MOI 50
MOI 100
E
SYN2
TH
Fold Change in gene expression
(Normalized to 0 dpt)
MOI 0
MOI 20
MOI 50
MOI 100
***
0 dpt
5 dpt
0 dpt
5 dpt

Figure 1

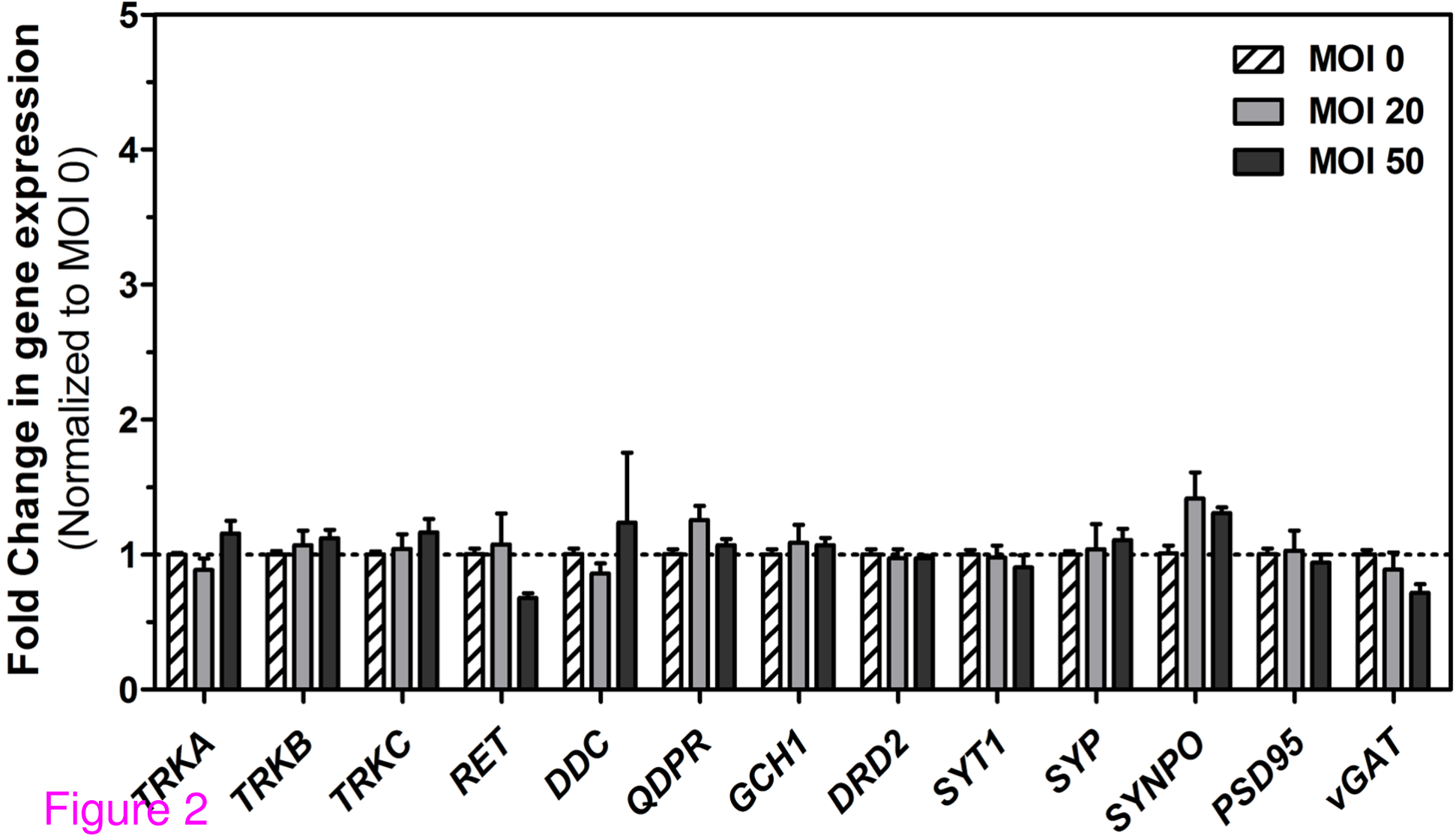
Fold Change in gene expression
(Normalized to MOI 0)
5
4
3
2
1
0
MOI 0
MOI 20
MOI 50
TRKA
TRKB
TRKC
RET
DDC
QDPR
GCH1
DRD2
SYT1
SYP
SYNPO
PSD95
vGAT

Figure 2

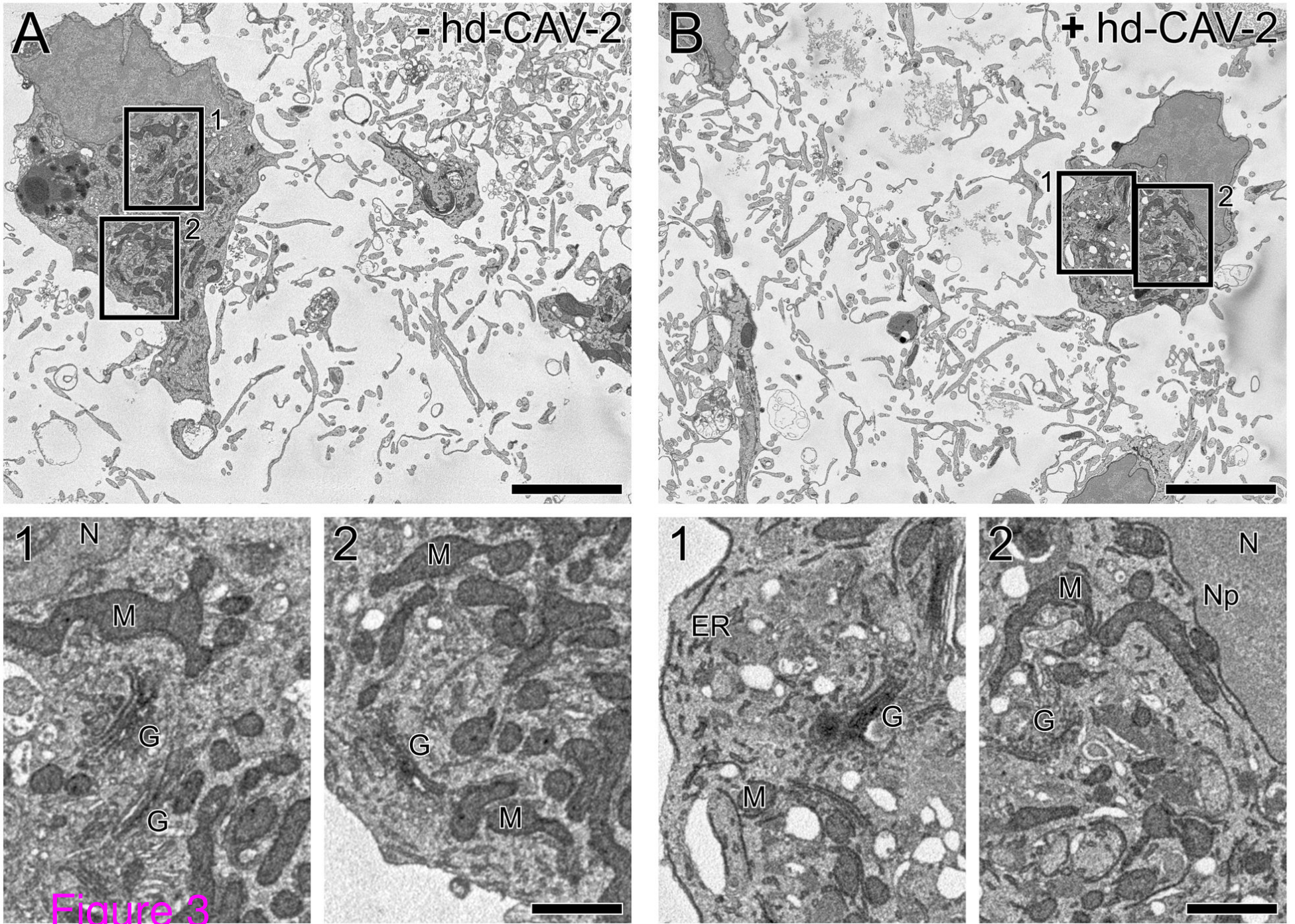

Figure 3

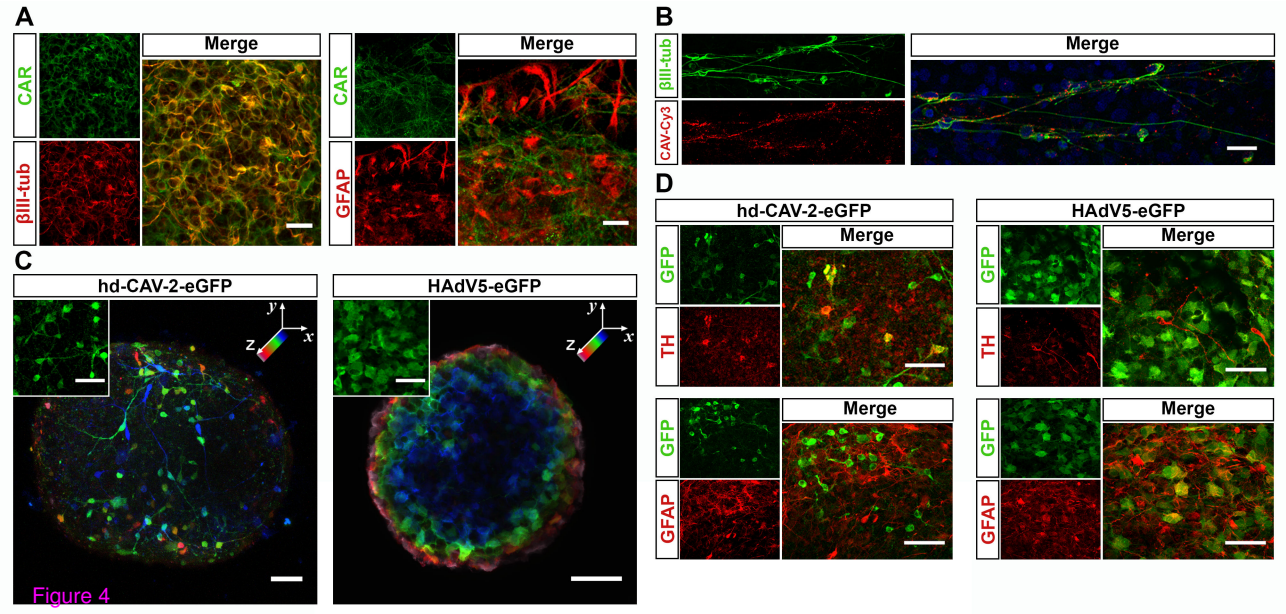
A
CAR
βIII-tub
Merge
CAR
GFAP
Merge
B
βIII-tub
CAV-Cy3
Merge
C
hd-CAV-2-eGFP
HAdV5-eGFP
y
x
z
D
hd-CAV-2-eGFP
HAdV5-eGFP
GFP
TH
GFAP
Merge
Figure 4

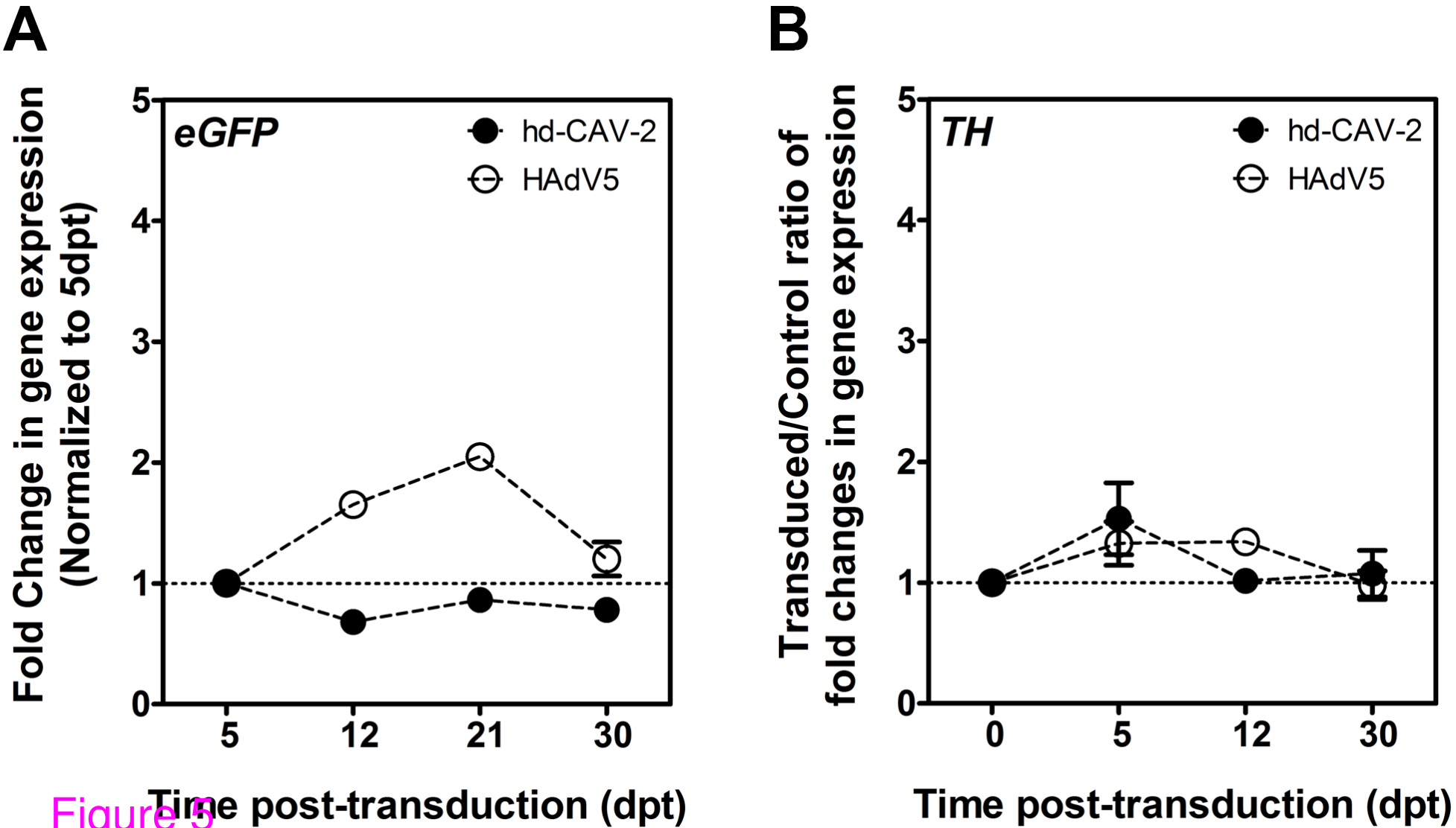
A
eGFP
hd-CAV-2
HAdV5
Fold Change in gene expression
(Normalized to 5dpt)
0
1
2
3
4
5
5
12
21
30
Time post-transduction (dpt)
B
TH
hd-CAV-2
HAdV5
Transduced/Control ratio of
fold changes in gene expression
0
1
2
3
4
5
0
5
12
30
Time post-transduction (dpt)

Figure 5

Additional files provided with this submission:

Additional file 1: VideoS1.mp4, 19304K
http://www.biomedcentral.com/imedia/3942531931642290/supp1.mp4
Additional file 2: VideoS2.m4v, 20045K
http://www.biomedcentral.com/imedia/1907236050164229/supp2.m4v